

Effect of Temperature on Physical Aging of Thin Glassy Polymer Films

Y. Huang and D. R. Paul*

Department of Chemical Engineering and Texas Material Institute, The University of Texas at Austin, Austin, Texas 78712

Received June 18, 2005; Revised Manuscript Received August 17, 2005

ABSTRACT: The effect of temperature on the kinetics of physical aging of thin films formed from two amorphous glassy polymers, polysulfone based on bisphenol A and poly(2,6-dimethyl-1,4-phenylene oxide), was investigated by monitoring the changes in gas permeability and refractive index. Films with different thicknesses were subjected to isothermal aging at three temperatures, ranging from 35 to 55 °C, for a period of aging of more than 200 days. The rate of permeability loss and the rate of densification determined from the refractive index change by using the Lorentz–Lorenz equation were found to increase with aging temperature. Similar qualitative trends of aging rate were noted by the two measurements. The combination of effects of aging temperature and film thickness on aging behavior were studied and compared with previous research.

Introduction

Physical aging, a phenomenon common to all amorphous materials in the glassy state, refers to the evolution toward an equilibrium state and the associated changes in physical properties at temperatures below the glass transition, T_g . Typical physical aging studies usually involve probing the relaxation of volume and enthalpy.¹ Tracking changes in gas permeability of polymer films is also a useful way of monitoring physical aging since permeability is quite sensitive to the loss of free volume;^{2–8} our recent work has shown the rate of permeability reduction during aging to depend on film thickness in addition to the chemical structure of the polymer.⁷ Indeed, films that are submicron in thickness age orders of magnitude more rapidly than expected for bulk glasses; this has considerable implications for commercial gas separation membranes. Ellipsometry of thin films has proven to be another sensitive way to track physical aging and provides a rather direct way, via the Lorentz–Lorenz equation, to follow the densification.⁹ Our prior work has been done at a single temperature, 35 °C;^{7,9} the objective here is to explore the effect of aging temperature (T_a) in conjunction with film thickness on the changes in gas permeability and optical properties.

It has been proposed that physical aging takes place in the temperature range between the β relaxation, T_β , and T_g , where T_β refers to the first (i.e., highest) secondary transition associated with the small-scale, subsegmental, local intramolecular motions about the flexible linkages in the polymer chain in the glass state.¹⁰ However, some evidence that physical aging is possible at temperatures below the β relaxation has been reported.¹¹ In any case, the β relaxations for the glassy polymers studied in this work are far below room temperature (see Table 1), and investigation of how these relaxations may affect the aging process is beyond the scope of this study.

The effect of film thickness on physical aging of glassy polymers of interest for gas separation began some years ago at the University of Texas at Austin. Pinnau first

Table 1. Bulk Physical Properties of Polymers Studied

polymer	ρ (g/cm ³)	T_g (°C)	T_β (°C)	n	f
PSF	1.240	186	$\sim -110^a$	1.633	0.1435
PPO	1.069	210	~ -50 to 0^b	1.573	0.1834

^a From refs 10 and 47. ^b From refs 45, 46, and 48.

compared the experimental results from asymmetric membranes with thick, dense films.² Pfromm and Koros concluded that membrane thickness plays an important role in aging; thin films from a fluorinated polyimide and bisphenol A polysulfone exhibited accelerated physical aging that was attributed to diffusion of free volume.³ Dorkenoo and Pfromm extended their studies using glassy thin films made from a polynorbornene and poly [1-(trimethylsilyl)-1-propyne] both experimentally and theoretically.^{12,13} Punsalan and Koros further studied the thickness-dependent sorption and effects of physical aging on a polyimide.¹⁴ McCaig and Paul^{6,15} investigated accelerated aging in thin polyarylate films in a more systematic way for films whose thicknesses ranged from 0.25 to 33 μm at a single temperature of 35 °C for a period of about 300 h. More recently, other research groups have begun to explore these issues using other techniques. For example, Priestly et al.¹⁶ reported studies on structural relaxation of ultrathin glassy polymer films which showed significant differences in the relaxation processes in the free surface layer, the interior of the ultrathin film, and the interface layer confined by the substrate; these differences seem to depend on aging temperature.

Recently, the effect of thickness on T_g has been widely studied for thin film systems with or without substrate confinement where the film thickness (l) is on a scale comparable to the size of the polymer coils ($l < 150$ nm).^{17–35} The thicknesses of thin films used in this work are much greater than this range, and it has been shown previously that the T_g of these thin films is the same as that observed in the bulk.^{7,36} Thus, the thickness-dependent aging phenomena described later do not seem to stem from a thickness effect on the glass transition temperature.

In this paper, three aging temperatures, 35, 45, and 55 °C, that are far below the respective T_g of each polymer are used to monitor the physical aging of thin

* To whom all correspondence should be addressed: e-mail drp@che.utexas.edu; Tel +1-512-471-5392; Fax +1-512-471-0542.

Table 2. Details of Film Formation

polymer	film thickness (μm)	formation method	solvent used
PSF	<5	spin-coating	cyclopentenone
	>5	solution-casting	dichloromethane
PPO	<5	spin-coating	chlorobenzene
	>5	solution-casting	trichloroethylene

glassy polymer films for up to 400 days. These temperatures were chosen on the basis of the limitation of the techniques and procedures used and the typical temperature range of interest to the gas separation industry. Most literature reports on physical aging do not use temperatures far below T_g because for bulk samples the aging response does not become significant on sensible time scales; however, this is not the case for thin films or for many asymmetric or composite gas separation membranes. From other studies,^{10,37–44} we can anticipate increased aging rates as the temperature is increased in the range considered here because the higher mobility enhances the rate of structural recovery.

Experimental Section

Materials. Two glassy polymers were used in this work: the polysulfone based on bisphenol A (PSF) and poly(2,6-dimethyl-1,4-phenylene oxide) (PPO). These materials have been described previously⁷ and were used as received. Their corresponding bulk values of T_g and T_β , density (ρ), refractive index (n), and fractional free volume (f) are listed in Table 1. The T_g values shown were experimentally determined in a conventional manner using a Perkin-Elmer DSC-7 differential scanning calorimeter upon heating using a cycle of heating at 20 °C/min and cooling at 40 °C/min. The sample was scanned twice, and the T_g reported represents the onset of the transition in the second scan. The T_β values were taken from the literature and were determined by dynamic mechanical analysis at frequencies in the range 11–110 Hz.^{10,45–48} Clearly, these values are far below the aging temperatures accessible by the current techniques. The densities and the refractive indices for PSF and PPO were obtained from the supplier, while the fractional free volume ($f = (V - V_o)/V$) was estimated from the specific volume ($V = 1/\rho$) and the occupied volume (V_o) computed by Bondi's method;⁴⁹ i.e., $V_o = 1.3V_w$, where V_w is the van der Waals volume computed by a group contribution method.⁵⁰ These volumes were determined at 25 °C.

Film Preparation. In this work, films with thicknesses less than 5 μm were made by spin-coating polymer solutions at a spinning speed of 1000 rpm for about 60 s onto the clean native oxide (100) surface of a silicon wafer. Films with thicknesses more than 5 μm were made by solution casting on the silicon wafer. The details of these methods have been described elsewhere⁵¹ and are summarized in Table 2. The film thickness was tuned by the concentration of the polymer solution which was filtered through a 0.1–0.45 μm Whatman PURADISC Teflon filter before coating/casting. The final dry film thickness was measured using different instruments. For films less than 2 μm , thickness was determined by ellipsometry.⁵¹ For films 2–10 μm thick, thickness was obtained using a profilometric device.^{7,51} A micrometer was used to measure the thicknesses of more than 10 μm . The thickness nonuniformity of all films was found to be in the range 0.5–3%. Films thicker than 25 μm may be assumed to exhibit "bulk" behavior. The film was removed from the wafer surface using deionized water and transferred onto a sample holder in a free-standing state; it was then equilibrated at a temperature of 15 °C above T_g for 40 min in an oven with a N_2 purge to remove prior thermal history and subsequently quenched rapidly to room temperature. The "fresh" film sample was then configured for permeation or refractive index measurement following the procedures described previously.^{7,9} These samples were isothermally aged in air in storage chambers thermostated at 35, 45, or 55 °C (fan-assisted) with measurement of gas perme-

ability and refractive index (see below for details) at certain times; after each measurement, the sample was returned to the original storage chamber for continued aging. The films prepared for permeation measurement had thicknesses up to 62 μm , and at least two duplicate samples were prepared for each film thickness; films used for the refractive index determination had thicknesses less than $\sim 1 \mu\text{m}$, and four duplicate samples were used to explore reproducibility.

Permeability Measurement. Pure gas permeability coefficients were measured at the same temperature as the aging temperature for O_2 , N_2 , and CH_4 at an upstream pressure of 2 atm using a constant-volume/variable-pressure type permeation cell following the standard procedures employed in this laboratory^{52,53} with specific details established for this work.^{7,51} During the aging process, the film samples were free-standing without significant interaction with the Anopore disk used as mechanical support during the permeation measurement. Isothermal experiments involved the sample being measured continuously as a function of aging time at the temperature used for sample storage. Two permeation cells were built to accommodate the two polymers studied which could be easily thermostated at the desired aging temperature.

Refractive Index Measurement. A variable angle spectroscopic ellipsometer (VASE), model 2000D, from J.A. Woolam was used to determine the refractive index of polymer films at room temperature (25 ± 0.1 °C). In contrast to permeability measurements, the refractive index was determined at room temperature after removal of the film sample from the aging storage chamber, regardless of the aging temperature. The details for the refractive index measurement have been given in an earlier paper.⁹ Ideally, the thin film should be free-standing during aging, which requires the film to be on and off the wafer surface before and after the refractive index measurement; however, such a procedure increases the probability of damaging the film sample after a few trials and decreases the precision of the ellipsometry measurement. The scheme used for permeation measurement where an Anopore support disk is employed does not work for the refractive index measurement because of the difficulty in making the film strictly flat on this support and poses serious alignment problems. The compromise adopted here was to have the thin films continuously on the silicon wafer surface during the aging process. This scheme is assumed to have little effect on physical aging since the polymer film was not constrained by the wafer support. There is only physical contact between the film and wafer surface, and the film could be easily removed by simply lifting it off the wafer. At least three ellipsometry measurements were conducted for each film sample, and the average value was computed to increase the accuracy and shown in the figures presented in this work. These three measurements could be completed within 5 min after removal from the aging chamber. Any alteration to physical aging during this short time caused by the measurement temperature, 25 °C, being different than the aging temperature, was assumed insignificant since the whole aging process persists for very long times.⁷

Results and Discussion

Effect of Aging Temperature As Tracked by Gas Permeability. Excellent reproducibility of the permeability measurement has been demonstrated previously with the maximum difference between the two duplicate samples less than 2.5% at any aging time. The permeability coefficients reported here are from a single film measurement.

Figure 1 shows an example of the permeability coefficients (P) for PSF films of various thicknesses as a function of the isothermal aging time (t) at 35 °C when both the aging and measurement temperatures were the same and held constant with a precision of ± 0.1 °C. Data were collected for periods up to 10 000 h depending on the aging temperature used. The aging behavior observed is similar to that published earlier,⁷ and

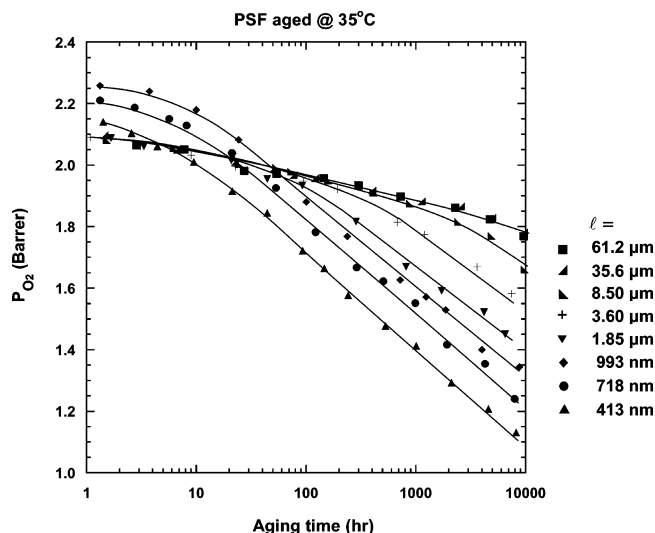


Figure 1. Evolution of oxygen permeability coefficients of PSF films of different thicknesses isothermally aged at 35 °C. Note that the unit “barrer” commonly used in the gas permeation literature has the following meaning: 1 barrer = 10^{-10} cm³ (STP) cm/(cm² s cmHg).

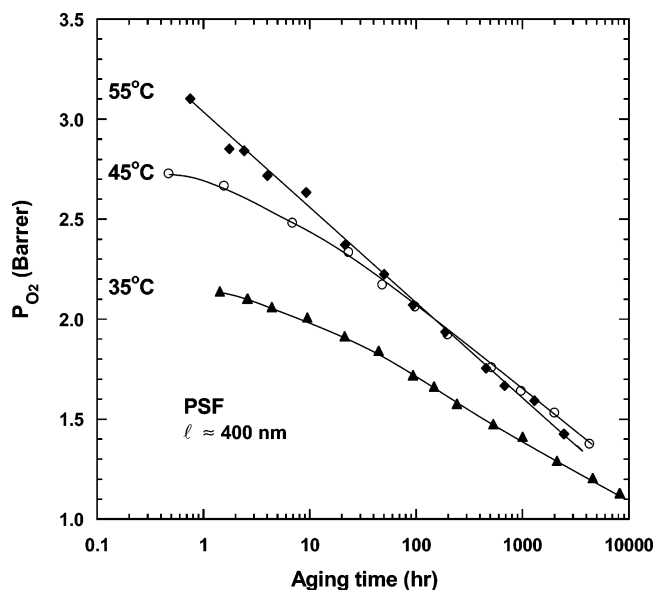


Figure 2. Absolute oxygen permeability of PSF films with thicknesses of ~400 nm as a function of aging time at the three aging temperatures.

similar trends were observed for other aging temperatures. Greatly accelerated physical aging is noted for thin films compared to thick films of the same polymer as reported previously;^{2–4,6,12,13,15} aging persists for long times with no evidence of reaching an equilibrium state. The vastly higher aging rate for thin films has been rationalized by the greater possibility of free volume diffusion and escape from the surface of thin polymer films compared to thicker ones.⁷

Figure 3 shows a comparison of how the evolution of oxygen permeability for PSF films with thickness of ~400 nm is affected by temperature. The higher permeability coefficients observed at higher temperature at the beginning of the aging process are expected due to the normal effect of temperature on permeability. The higher the temperature, the more rapidly gas permeability is observed to decrease during aging. For example, Figure 2 shows that at 55 °C the permeability drops to values lower than observed at 45 °C after an

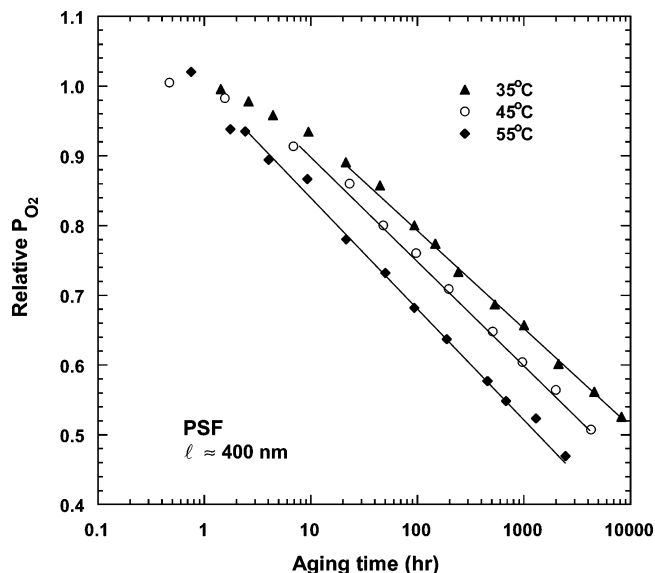


Figure 3. Relative oxygen permeability of PSF films with thicknesses of ~400 nm (normalized by value at $t = 1$ h) as a function of aging time at three aging temperatures.

aging time of ~100 h. To more directly compare the aging response at different temperatures, the oxygen permeability coefficients are replotted in Figure 3 normalized by the value observed at 1 h as a function of aging time for each temperature. By this measure, at any time after 1 h, the relative oxygen permeability is lower the higher the aging temperature. This suggests that aging rate increases with temperature as might be expected on the basis of mobility considerations. The relationships in Figure 3 display a rather wide time interval over which an approximate linear relationship pertains; however, there is clearly a delay before the apparent linear range is reached, and with reducing aging temperature, this “delay time” increases. This phenomenon is reminiscent of volumetric aging results on atactic polystyrene reported by Hutchinson,¹ who described the time to reach this linear region as the inflection point. The time scale for the delay obtained here is comparable to the values reported in the literature for aging temperatures far below T_g .^{1,54} The slope of the approximate linear region decreases with decreasing temperature as might be expected; however, the effect is not large for these relatively small temperature differences. Similar results were obtained for films with other thicknesses.

In an earlier paper we characterized aging rate in terms of the slope of plots of $\log P$ vs $\log t$ (e.g., Figure 4) as is commonly done in the membrane industry; such plots yield a nearly linear relationship at long aging times.⁷ For the plots in Figure 4, it seems that the approximately linear relationship develops after aging times of ~100 h. Figure 5 shows how this measure, i.e., $-(\partial \log P_{O_2} / \partial \log t)$, of aging rate depends on film thickness and aging temperature for PSF films. These plots indicate that at each temperature the rate of permeability loss with aging decreases as the film thickness increases and appears to level off as the film approaches what might be considered the bulk state, as reported earlier.⁷ The rate of permeability reduction is higher the higher the aging temperature. The effect of thickness on the oxygen permeability reduction rate appears to diminish as aging temperature increases; i.e., the influence of film thickness on physical aging seems to moderate at high aging temperatures. The coupling

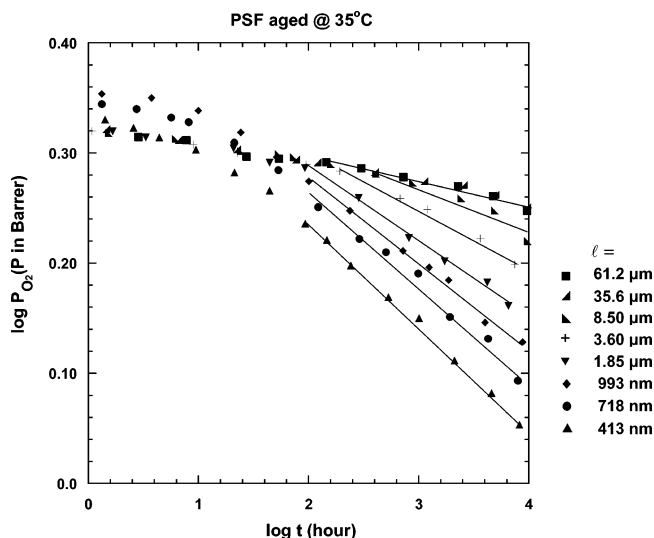


Figure 4. Logarithmic plots of the oxygen permeability and aging time for PSF films aged at 35 °C. An approximately linear relationship develops after an aging time of ~ 100 h.

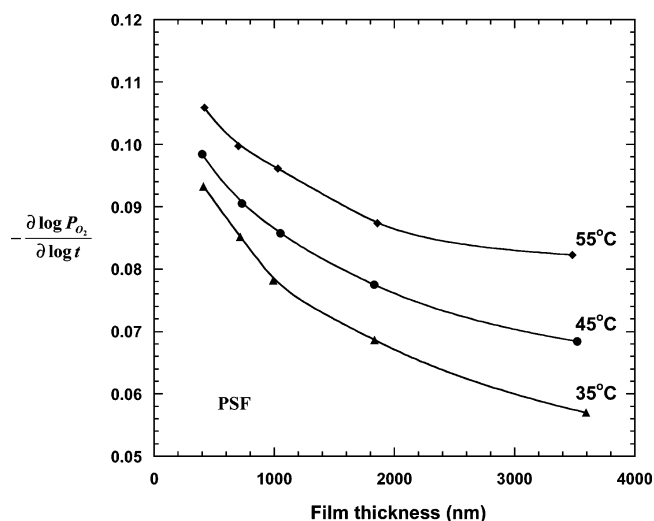


Figure 5. Rate of change of oxygen permeability at long aging times for PSF films as a function of film thickness at different aging temperatures.

effect of film thickness and aging temperature is also noted in the studies of relaxation dynamics of glasses below the glass transition by Jérôme and Comman-deur⁵⁵ for ultrathin films.

The observations noted above for PSF are similar to those observed for PPO film samples aged at these temperatures. Figure 6 summarizes the oxygen permeability reduction rate for both PSF and PPO films as a function of aging temperature. Clearly, PPO shows a much higher aging rate than PSF. The aging rate is not a linear function of the aging temperature, and PSF seems to be more sensitive to the aging temperature than PPO; as the temperature is increased from 35 to 55 °C, the oxygen permeability reduction rate for films with thickness of ~ 400 nm increased 13.5% for PSF compared to 6.4% for PPO. It is significant to note that PPO has a much higher free volume than PSF does. We believe this is a key element that determines the relative rate of aging of one polymer vs another at a given thickness at aging temperatures far below T_g ; this idea will be explored more fully in future studies.

Effect of Aging Temperature as Tracked by Refractive Index. Good reproducibility of the refrac-

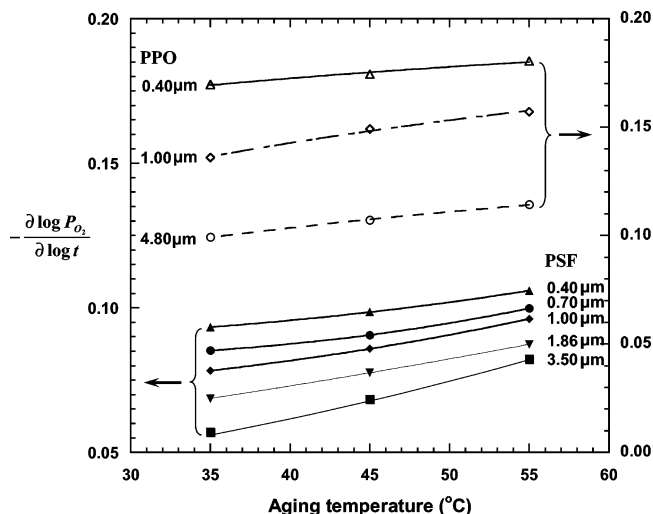


Figure 6. Comparison of the rate of change of oxygen permeability for PSF and PPO films of different thickness as a function of aging temperature. Closed symbols correspond to films made from PSF while the open symbols represent films made from PPO.

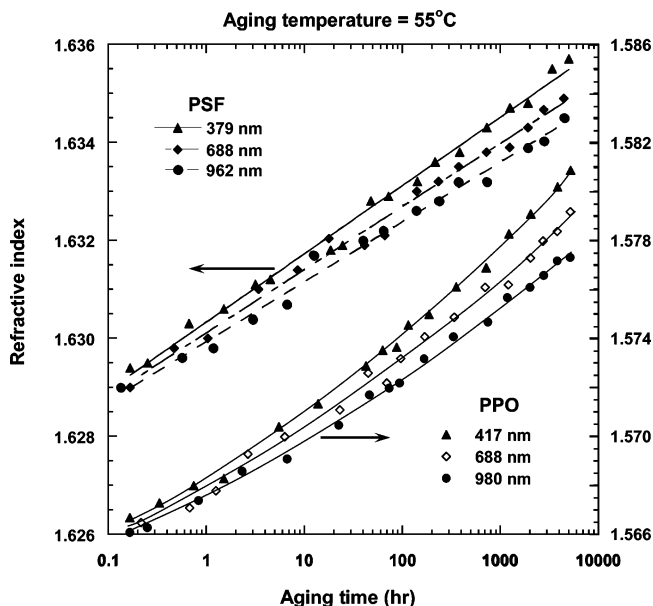


Figure 7. Change in the refractive index of PSF and PPO thin films with time at 55 °C. Closed symbols correspond to films made from PSF while the open symbols represent films made from PPO.

tive index measurement has also been shown in an earlier paper with the maximum difference among the duplicate samples less than 0.05% at any aging time.⁹ The refractive index shown in the following figures is the average of multiple measurements for a single film; the variation among these values is less than 7×10^{-5} for all films at any aging time.

Figure 7 shows the change of the refractive index (measured at 25 °C) of PSF and PPO thin films with aging time at 55 °C. For PSF, an approximately linear relationship is exhibited between the refractive index and $\log t$, except during the initial stages of aging. For PPO, the plots show some curvature for the aging period of investigation; nonetheless, the linear fit of the experimental data produces a correlation coefficient of $R^2 = 0.986$ for all PPO thin films. The slight scattering of the data about the trend of the refractive index change for each film might be considered as the error

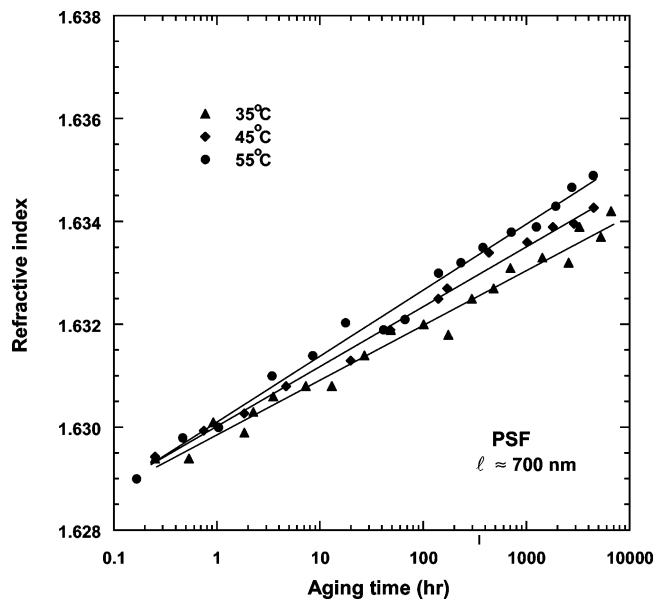


Figure 8. Change in refractive index of PSF films with thickness ~ 700 nm at different aging temperatures as a function of aging time.

of the measurement which is less than 0.0006 refractive index units for all films. In each case, thin films display a more rapid increase in refractive index than thick films as reported recently.⁹ Figure 8 shows the response of the refractive index measurement at 25 °C for PSF films (with thickness about 700 nm) aged at different temperatures. Clearly, the refractive index increases more rapidly the higher the aging temperature; this is consistent with the gas permeability changes shown in the last section.

The Lorentz–Lorenz equation⁹

$$L = \frac{n^2 - 1}{n^2 + 2} = \frac{\rho N_{av} \alpha}{3M_0 \epsilon_0} = \rho C \quad (1)$$

provides a connection between refractive index and density, where N_{av} is Avogadro's number, M_0 is the molecular weight of the polymer repeat unit, ϵ_0 is the permittivity of free space constant, ρ , and α is the average polarizability of the polymer repeat unit. The parameters on the right-hand side of the Lorentz–Lorenz equations are constant except for density⁹ and are summarized into the material constant C , i.e., $C = N_{av} \alpha / 3M_0 \epsilon_0$. Since the refractive index appears to be an approximately linear function of $\log t$, the Lorentz–Lorenz parameter, L , should also be an approximately linear function of $\log t$, due to the fact that the change in refractive index during aging is quite small, as seen in Figure 7. Likewise, $\log L$ approximately linearly correlates with $\log t$, as demonstrated in Figure 9 for PSF thin films aged at 45 °C. As shown previously, the Lorentz–Lorenz equation also provides a simple way to define a volumetric aging rate,⁹ i.e.

$$r = \left(\frac{\partial \log L}{\partial \log t} \right)_{P,T} = \left(\frac{\partial \log \rho}{\partial \log t} \right)_{P,T} \quad (2)$$

The volumetric aging rate was calculated for each polymer film at each aging temperature from the slope of a log–log plot of L vs aging time within the region over which such plots are best linearly fitted. Figure 10 shows how this volumetric aging rate depends on film thickness and aging temperature for PSF. At a given

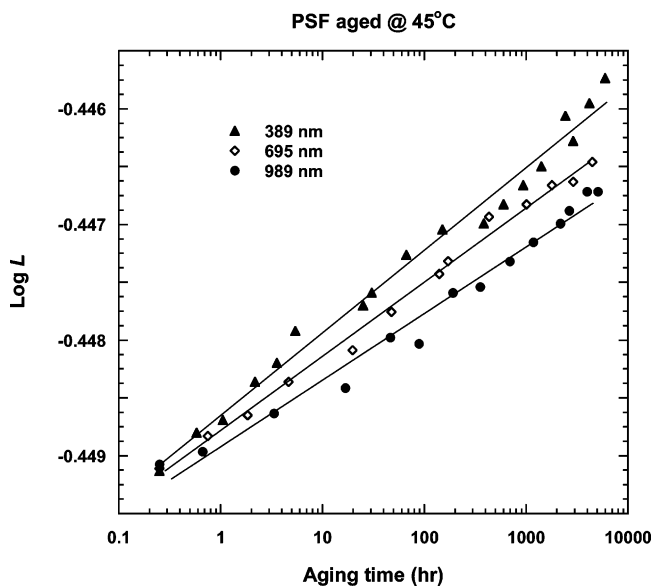


Figure 9. A log–log plot of Lorentz–Lorenz parameter vs aging time for PSF thin films aged at 45 °C.

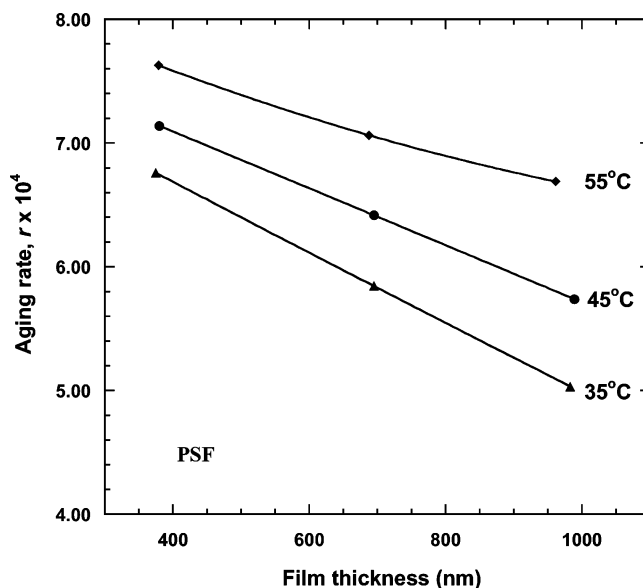


Figure 10. Volumetric aging rate, r , determined from the Lorentz–Lorenz equation vs film thickness for PSF films at different temperatures.

thickness the aging rate increases with aging temperature; the aging rate decreases as the film thickness increases at each aging temperature, and the influence of thickness on aging rate seems to be more apparent at lower temperatures, in agreement with the observations by gas permeability. These optically determined volumetric aging rates at temperatures more than 100 °C below T_g are higher than those reported in the literature for bulk polymers aged at ~ 15 °C below T_g .^{1,56} Figure 11 compares the volumetric aging rate for PSF and PPO films, with thicknesses of about 400 nm, as a function of the inverse aging temperature. At a fixed thickness, PPO has a higher aging rate than PSF which is believed to reflect the higher fractional free volume of PPO.⁷ Figure 11 also shows that the effect of temperature on the aging rate can be approximated by an Arrhenius-like form. For films of ~ 400 nm in thickness, the apparent “activation energy” is 5.1 kJ/mol for the volumetric relaxation rate of PSF and 2.2 kJ/mol for

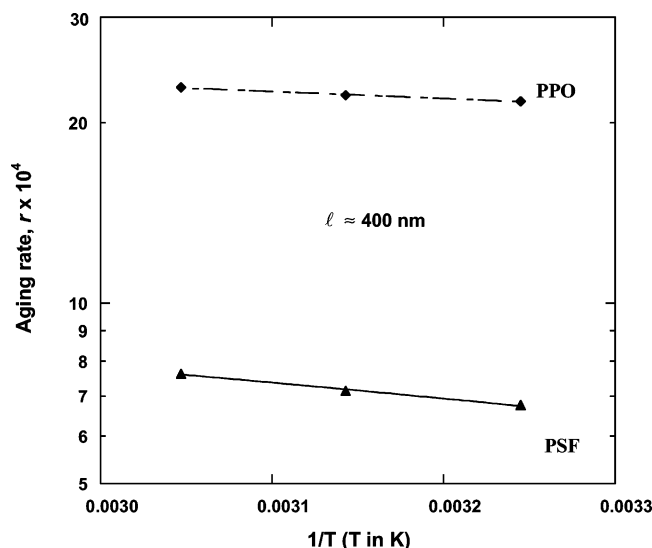


Figure 11. Volumetric aging rate, r , determined from the Lorentz–Lorentz equation vs aging temperature, for PSF and PPO films with thickness ~ 400 nm plotted on Arrhenius coordinates.

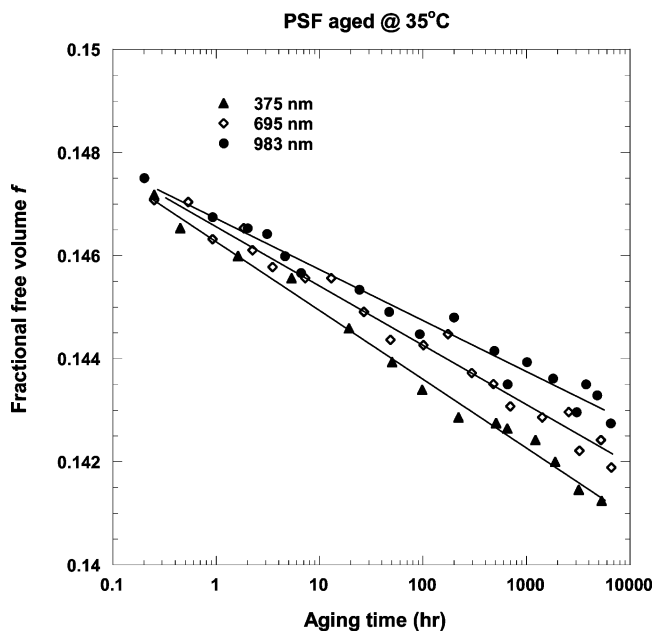


Figure 12. Change in fractional free volume with time for PSF films aged at 35 °C.

PPO, consistent with the fact that PPO ages more rapidly than PSF.

The material constant C in eq 1 can be obtained from the bulk values of refractive index and density for each polymer (given in Table 1). With this simple relationship, the density at any aging time can be calculated from the measured refractive index. In addition, the fractional free volume, f , at each stage of the aging process can be determined as follows:

$$f = \frac{V - V_0}{V} = 1 - \rho V_0 = 1 - \frac{L}{C} V_0 \quad (3)$$

Figure 12 presents an example of the fractional free volume obtained in this way for PSF films aged at 35 °C. The fractional free volume decreases gradually with aging time and at a higher rate for thin films than thick films, as expected.

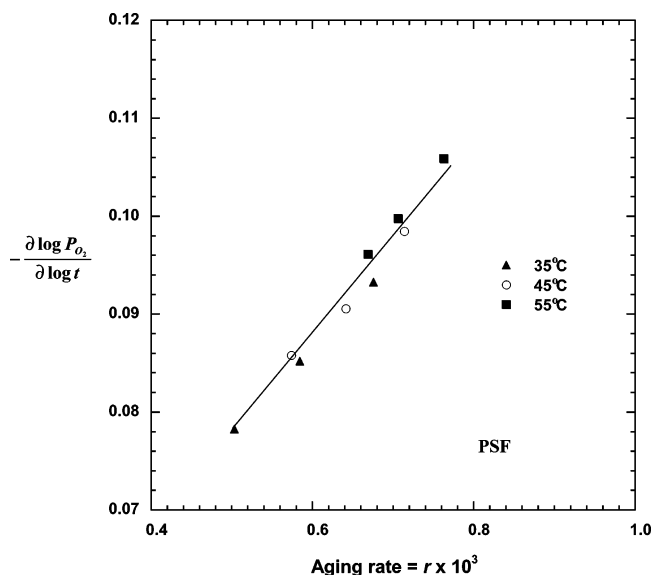


Figure 13. Correlation between oxygen permeability reduction rates and volumetric relaxation rates for PSF films with thicknesses less than $\sim 1 \mu\text{m}$.

Correlation of Aging Rates. Both of the measurement techniques employed in this work reflect the densification or reduction in polymer free volume during aging; therefore, as expected, both measurements provide similar descriptions of the aging behavior. It is, thus, expected that there may be a quantitative correlation between the two measures of aging rate. Figure 13 summarizes the oxygen permeability reduction rate vs the corresponding volumetric relaxation rate for all thin films, of thickness less than $\sim 1 \mu\text{m}$, of PSF aged at the three temperatures. Only data for thin films are shown since ellipsometry cannot be used to measure thick films; the upper limit of film thickness with sufficient measurement accuracy is about $1 \mu\text{m}$. An excellent correlation between the two measures of aging rate is seen. Similar correlations of aging rates obtained from positron annihilation, dielectric relaxation, and dynamic mechanical thermal analysis have also been reported.³⁹ More detailed data analysis for other polymers will be explored in future papers.

Summary and Conclusions

The observations reported here for PSF and PPO films agree qualitatively with the temperature dependence of the rate of volume relaxation reported in the literature.^{38,39,57} The results indicate that the aging rates determined by both oxygen permeability reduction and optically measured volume relaxation depend on both thickness and aging temperature; the aging process is faster the higher the aging temperature and the thinner the film. The Lorentz–Lorentz parameter appears to change linearly with aging time on a log–log plot and provides a direct correlation to the classical volumetric relaxation.⁹ Gas permeability measurements show a similar linear relation, on a log–log plot, but only at long aging times which provides a useful measure of the aging rate for comparison purposes. For both measurements, the aging rate increases with aging temperature for a particular film thickness. The effect of thickness on the aging response of polymer films seems to moderate at higher temperatures. The combined effects of thickness and temperature on the aging behavior are very similar to the results obtained by

Jérôme and Commandeur.⁵⁵ The similarity of response by both methods is further illustrated by a correlation between the two measures of aging rate; detailed data analyses involving different polymer types will be explored in future papers.

Acknowledgment. This research was supported by the Separations Research Program at the University of Texas at Austin and the National Science Foundation Grant DMR-0238979 administered by the Division of Material Research–Polymer Program.

References and Notes

- Hutchinson, J. M. *Prog. Polym. Sci.* **1995**, *20*, 703–760.
- Pinnau, I.; Koros, W. J. *J. Appl. Polym. Sci.* **1991**, *43*, 1491–1502.
- Pfromm, P. H.; Koros, W. J. *Polymer* **1995**, *36*, 2379–2387.
- Chung, T. S.; Kafchinski, E. R. *J. Appl. Polym. Sci.* **1996**, *59*, 77–82.
- Chung, T. S.; Teoh, S. K. *J. Membr. Sci.* **1999**, *152*, 175–188.
- McCaig, M. S.; Paul, D. R. *Polymer* **2000**, *41*, 629–637.
- Huang, Y.; Paul, D. R. *Polymer* **2004**, *45*, 8377–8393.
- Zhou, C.; Chung, T.-S.; Wang, R.; Goh, S. H. *J. Appl. Polym. Sci.* **2004**, *92*, 1758–1764.
- Huang, Y.; Paul, D. R. Submitted for publication.
- Struik, L. C. E. *Physical Aging in Amorphous Polymers and Other Materials*; Elsevier Scientific Publishing Co.: New York, 1978.
- Lee, H. H. D.; McGarry, F. J. *J. Macromol. Sci., Phys.* **1990**, *B29*, 11–29.
- Dorkenoo, K. D.; Pfromm, P. H. *J. Polym. Sci., Part B: Polym. Phys.* **1999**, *37*, 2239–2251.
- Dorkenoo, K. D.; Pfromm, P. H. *Macromolecules* **2000**, *33*, 3747–3751.
- Punsalan, D.; Koros, W. J. *J. Appl. Polym. Sci.* **2005**, *96*, 1115–1121.
- McCaig, M. S.; Paul, D. R.; Barlow, J. W. *Polymer* **2000**, *41*, 639–648.
- Priestley, R. D.; Ellison, C. J.; Broadbelt, L. J.; Torkelson, J. M. *Science* **2005**, *309*, 456–459.
- Kim, J. H.; Jang, J.; Lee, D. Y.; Zin, W.-C. *Macromolecules* **2002**, *35*, 311–313.
- Kim, J. H.; Jang, J.; Zin, W.-C. *Langmuir* **2000**, *16*, 4064–4067.
- Grohens, Y.; Sacristan, J.; Hamon, L.; Reinecke, H.; Mijangos, C.; Guenet, J. M. *Polymer* **2001**, *42*, 6419–6423.
- Pham, J. Q.; Green, P. F. *Macromolecules* **2003**, *36*, 1665–1669.
- Kawana, S.; Jones, R. A. L. *Phys. Rev. E* **2001**, *63*, 021501/1–021501/6.
- Beaucage, G.; Composto, R.; Stein, R. S. *J. Polym. Sci., Part B: Polym. Phys.* **1993**, *31*, 319–326.
- Keddie, J. L.; Jones, R. A. L.; Cory, R. A. *Europhys. Lett.* **1994**, *27*, 59–64.
- Keddie, J. L.; Jones, R. A. L. *Isr. J. Chem.* **1995**, *35*, 21–26.
- Grohens, Y.; Brogly, M.; Labbe, C.; David, M. O.; Schultz, J. *Langmuir* **1998**, *14*, 2929–2932.
- Orts, W. J.; van Zanten, J. H.; Wu, W. L.; Satija, S. K. *Phys. Rev. Lett.* **1993**, *71*, 867–870.
- Wu, W.; van Zanten, J. H.; Orts, W. J. *Macromolecules* **1995**, *28*, 771–774.
- Wallace, W. E.; van Zanten, J. H.; Wu, W. L. *Phys. Rev. E* **1995**, *52*, R3329–R3332.
- Forrest, J. A.; Dalnoki-Veress, K.; Stevens, J. R.; Dutcher, J. R. *Phys. Rev. Lett.* **1996**, *77*, 2002–2005.
- Forrest, J. A.; Dalnoki-Veress, K.; Dutcher, J. R. *Phys. Rev. E* **1997**, *56*, 5705–5716.
- Xie, L.; DeMaggio, G. B.; Frieze, W. E.; DeVriesd, J.; Gidley, D. W.; Hristov, H. A.; Yee, A. F. *Phys. Rev. Lett.* **1995**, *74*, 4947–4950.
- DeMaggio, G. B.; Frieze, W. E.; Gidley, D. W.; Zhu, M.; Hristov, H. A.; Yee, A. F. *Phys. Rev. Lett.* **1997**, *78*, 1524–1528.
- Fukao, K.; Miyamoto, Y. *Phys. Rev. E* **2000**, *61*, 1743–1754.
- Fukao, K.; Uno, S.; Miyamoto, Y.; Hoshino, A.; Miyaji, K. *Phys. Rev. E* **2001**, *64*, 051807/1–051807/1.
- Fukao, K.; Miyamoto, Y. *Phys. Rev. E* **2001**, *64*, 011803/1–011803/9.
- Huang, Y. Ph.D. Dissertation, Chemical Engineering, The University of Texas at Austin, Austin, 2005.
- Petrie, S. E. B. *J. Polym. Sci., Polym. Phys. Ed.* **1972**, *10*, 1255–1272.
- Drozdov, A. D. *J. Appl. Polym. Sci.* **2001**, *81*, 3309–3320.
- Davis, W. J.; Pethrick, R. A. *Polymer* **1998**, *39*, 255–266.
- Chow, T. S. *Macromolecules* **1992**, *25*, 440–444.
- Royal, J. S.; Victor, J. G.; Torkelson, J. M. *Macromolecules* **1992**, *25*, 729–734.
- Royal, J. S.; Torkelson, J. M. *Macromolecules* **1993**, *26*, 5331–5335.
- Alegria, A.; Goitiandia, L.; Telleria, I.; Colmenero, J. *Macromolecules* **1997**, *30*, 3881–3887.
- Priestley, R. D.; Broadbelt, L. J.; Torkelson, J. M. *Macromolecules* **2005**, *38*, 654–657.
- Stoelting, J.; Karasz, F. E.; MacKnight, W. J. *Polym. Eng. Sci.* **1970**, *10*, 133.
- Eisenberg, A.; Cayrol, B. *J. Polym. Sci., Part C* **1971**, *35*, 129.
- Drzewinski, M.; MacKnight, W. J. *J. Appl. Polym. Sci.* **1985**, *30*, 4.
- Aguilar-Vega, M.; Paul, D. R. *J. Polym. Sci., Part B: Polym. Phys.* **1993**, *31*, 1577–1589.
- Bondi, A. *Physical Properties of Molecular Crystals, Liquids and Glasses*; Wiley: New York, 1968.
- van Krevelen, D. W. In *Properties of Polymers: Their Correlation with Chemical Structure, Their Numerical Estimation and Prediction from Additive Group Contributions*, 3rd completely rev. ed.; Elsevier: Amsterdam, 1990.
- Huang, Y.; Paul, D. R. *J. Membr. Sci.* **2004**, *244*, 167–178.
- Barbari, T. A.; Koros, W. J.; Paul, D. R. *J. Polym. Sci., Part B: Polym. Phys.* **1988**, *26*, 709–727.
- McHattie, J. S.; Koros, W. J.; Paul, D. R. *Polymer* **1991**, *32*, 840–850.
- Kovacs, A. J. *Fortschr. Hochpolym. Forsch.* **1964**, *3*, 394–508.
- Jérôme, B.; Commandeur, J. *Nature (London)* **1997**, *386*, 589–592.
- Robertson, C. G.; Wilkes, G. L. *Polymer* **1998**, *39*, 2129–2133.
- Cowie, J. M. G.; Harris, S.; McEwen, I. J. *Macromolecules* **1998**, *31*, 2611–2615.

MA051284G